Targeting stromal interactions in the pro-metastatic tumor microenvironment : Endoglin & TGF-beta as (un)usual suspects

Paauwe, M.

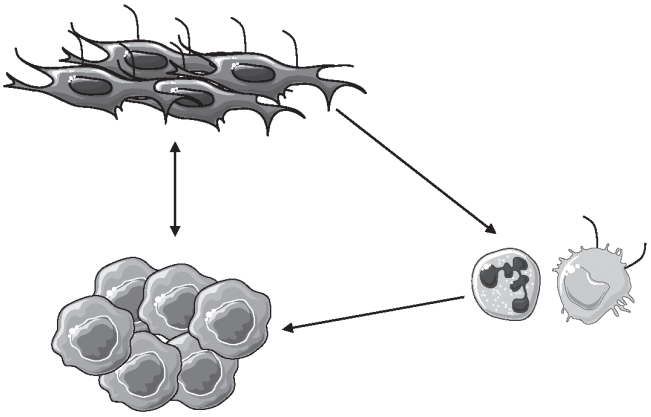

Chapter 8

Fibroblast-specific endoglin knock out increases formation of intestinal pre-malignant lesions

Madelon Paauwe[1,2], Mark J.A. Schoonderwoerd[2], Lars Ottevanger[2], Eveline S.M. de Jonge-Muller[2], Marie-José Goumans[1], Marieke F. Fransen[3], James C.H. Hardwick[2], Peter ten Dijke[1,4], Lukas J.A.C. Hawinkels[1,2]

[1]Dept. of Molecular Cell Biology, [2]Dept. of Gastroenterology-Hepatology, [3]Immunohematology and Blood Transfusion, Leiden University Medical Center, Leiden, The Netherlands
[4]Ludwig Institute for Cancer Research, Uppsala University, Uppsala, Sweden

Manuscript in preparation

Abstract

Disruption of the intricate balance in paracrine communication between epithelial cells and intestinal stromal cells disturbs intestinal homeostasis and can result in spontaneous polyp formation. As during homeostasis, interactions between epithelial tumor cells and the tumor stroma play an important often pro-tumorigenic role during colorectal cancer (CRC) progression. Previously, we showed the importance of the transforming growth factor-β (TGF-β) co-receptor endoglin on cancer-associated fibroblasts (CAFs) in CRC metastasis, suggesting a role in the interaction between tumor cells and CAFs. To determine the role of endoglin on fibroblasts in intestinal tumorigenesis, we generated a tamoxifen-inducible, fibroblast-specific endoglin knock out mouse. Tumor formation was induced using azoxymethane followed by dextran sodium sulphate (AOM/DSS). We observed a high increase in the number of AOM/DSS-induced lesions upon fibroblast-specific endoglin deletion. Lesion size was not affected by endoglin deletion. In lesions from endoglin knockout mice, both total stroma content and the number of activated fibroblasts were increased, although this did not affect total collagen deposition. Additionally, increased infiltration of macrophages and neutrophils in tumors was observed. Moreover, expression profiles of immunoregulatory genes were changed in endoglin knock out fibroblasts *in vitro* and in lesions from mice after fibroblast-specific endoglin deletion. Together, these data suggest an important role for endoglin on fibroblasts during tumorigenesis, possibly via altered recruitment of macrophages and neutrophils.

Introduction

The intestinal epithelium is very dynamic, with a high proliferation rate in the colonic crypts and differentiation and apoptosis at the luminal surface of the intestine (*1, 2*). This homeostatic process is tightly regulated by paracrine signaling between epithelial and stromal cells in the intestine. Major players in intestinal homeostasis are the bone morphogenetic protein/transforming growth factor-β (BMP/TGF-β) and Wnt signaling pathways (*3-6*).

As for intestinal homeostasis, paracrine interactions between malignant epithelial cells and their microenvironment play a crucial role in colorectal cancer (CRC) progression and metastatic spread (*7, 8*). The tumor microenvironment (TME), consists of endothelial cells, immune cells and cancer-associated fibroblasts (CAFs) (*9*). CAFs are a main component of the TME and have been shown to be involved in tumor progression and invasiveness, e.g. by remodeling the extracellular matrix (ECM), secreting proteases and regulating the immune status of the tumor (*10-12*). CAFs are a heterogeneous cell population with a fibroblast morphology, expressing vimentin, α-Smooth Muscle Actin (αSMA) and fibroblast activation protein (FAP) (*13*). Although extensively studied, the cell-of-origin of CAFs is still under debate. One commonly accepted hypothesis is that local fibroblasts are activated under the influence of tumor-derived cytokines, mainly TGF-β (*14-16*).

The TGF-β co-receptor endoglin is highly expressed on activated endothelium and was shown to be indispensable for developmental angiogenesis (*17-19*). In endothelial cells, endoglin is involved in signal transduction of its ligands TGF-β and BMP-9 (*20, 21*), ultimately leading to a pro-angiogenic phenotype, characterized by increased endothelial proliferation and migration (*22-25*).

We and other groups have observed that, next to endothelial cells, endoglin is expressed on CAFs, mainly at the invasive borders of solid tumors (chapter 7). Endoglin on CAFs can play an important role in CRC metastasis, which is further strengthened by the fact that treatment with the endoglin neutralizing antibody TRC105 decreased metastatic spread in an *in vivo* model for CRC metastasis, rendering endoglin on CAFs a potential therapeutic target in CRC (chapter 7).

In this project we addressed the role of endoglin on fibroblasts during CRC initiation and progression, using the azoxymethane/dextran sodium sulphate (AOM/DSS) model (*26*). This most commonly used model for colitis-associated cancer generates tumors which show resemblance to human CRC (*27*).

We generated a tamoxifen-inducible collagen1α1-specific endoglin knock out mouse ($ENG^{Fib-/-}$). When we chemically induced tumor formation, a significant increase in the number of lesions was observed in $ENG^{Fib-/-}$ mice, when compared with control mice. Tissue analysis and *in vitro* experiments revealed that collagen1α1-specific, further referred to as fibroblast-specific, endoglin knock out resulted mainly in an expansion of the stromal compartment of lesions. Moreover, deletion of endoglin in fibroblasts resulted in enhanced recruitment of macrophages and neutrophils to AOM/DSS-induced lesions. Together, these

data imply that endoglin expression on fibroblasts might play a role in initiation of CRC, potentially by regulating immune cell infiltrate in early lesions.

Materials and methods

Cell culture, preparation of CM and signaling assays

Mouse fibroblasts and the mouse CRC cell line MC38 (*28*) were cultured in in DMEM/F12, supplemented with 10% fetal calf serum (FCS), 10 mM HEPES, 50 µg/mL gentamycin, 100 IU/mL penicillin and 100 µg/mL streptomycin (all ThermoFisher, Waltham, MA, USA). Mouse CRC cell line CT26 (*29*) was maintained in RPMI 1640, supplemented with 10% FCS, 100 IU/mL penicillin and 100 µg/mL streptomycin (all ThermoFisher). Murine embryonic fibroblasts (MEFs) were obtained from E12.5 embryos as described before (*30*), from an endoglin flox/flox mouse strain in which exons 5 and 6 are flanked by LoxP sites (*31*). MEFs and the mouse myoblast cell line C2C12 were maintained in DMEM, supplemented with 10% fetal calf serum (FCS), 100 IU/mL penicillin and 100 µg/mL streptomycin (all ThermoScientific). Constructs expressing Cre recombinase (pLV.mPGK.iCRE.IRES.PuroR, kindly provided by Dr. M. Goncalves, Dept. Molecular Cell Biology, Leiden University Medical Center) or an empty vector control were delivered using lentiviral transduction using polybrene (4 µg/mL, Hexadimethrine bromide, Sigma Aldrich) to 80% confluent MEFs and after 48 hours, transduced cells were selected by 1.5 µg/mL puromycin (Sigma Aldrich).

Conditioned medium (CM) from MEFs was prepared by serum starving subconfluent cells for four days. CM used for proliferation assays was two-fold diluted with culture medium, containing 5% FCS.

BMP signaling was determined using a Bre-Luc reporter construct as described earlier (*32*) and TGF-β signaling was assessed as described before (*8*). In short, MC38 or C2C12 cells were transfected using polyethylenimine (PEI; Polysciences Inc., Warrington, PA, USA). After four hours, medium was changed to normal culture medium and the next day cells were serum-starved overnight. Cells were stimulated with 5 ng/mL TGF-β (*33*), 100 ng/mL BMP-6 (PeproTech, London, UK), or conditioned medium from MEFs. After 6 hours of stimulation, cells were washed, lysed and luciferase activity was measured according to manufacturers' instructions (Promega, Leiden, The Netherlands).

MTS proliferation assay

5000 CT26 or MC38 cells were seeded in 96-well plates in triplicate. After 16 hours, medium was replaced with 100 µL CM, from either control or endoglin knock out MEFs or with non-conditioned medium. At indicated time points 20 µL MTS substrate (Promega, Madison, WI, USA) was added to each well and absorbance was measured at 490 nm using a VersaMax plate reader (Molecular Devices, Sunnyvale, CA, USA).

Mice

All animal experiments were approved by the Dutch animal ethics committee. Next to its expression in osteoblasts (*34*), collagen1α1 is expressed in fibroblasts (*35-37*), including those of the intestine (*38*). In this study we have used the collagen1α1 promoter in order to delete endoglin from fibroblasts, without affecting its expression on endothelial cells. Collagen1α1-CreERT2 mice were purchased from Jackson Laboratory (strain B6.Cg-Tg(Col1a1-cre/ERT2)1Crm, Bar Harbor, ME, USA). ENG*fl/fl* mice in which exons 5 and 6 of the endoglin gene are flanked by LoxP sites were generated by Allinson et al. (*31*). Before tamoxifen induction mice were divided into two groups, based on sex and body weight. Cre-mediated recombination was induced at 8 weeks of age by oral administration of 50 uL tamoxifen (100 μg/mL, Sigma-Aldrich, Zwijndrecht, The Netherlands) dissolved in sunflower oil, on three consecutive days. Control mice had the same genotype, but were not treated with tamoxifen. Collagen1α1-CreERT2.ENG*fl/fl* and ENG*fl/fl* mice were used for control experiments as described. Mice were genotyped by PCR for the presence of the Cre recombinase and endoglin LoxP gene using the following primers; Cre recombinase Fw 5'-ACGAGTGATGAGGTTCGCAA -3', Cre recombinase Rev 5'-AGCGTTTTCGTTCTGCCAAT -3', endoglin LoxP Fw 5'-CCACGCCTTTGTCCTTGC-3', endoglin LoxP Rev 5'-GACGCCATTCTCATCCTGC-3' (all Invitrogen Carlsbad, CA, USA).

AOM/DSS model

Two weeks after tamoxifen induction male and female Collagen1α1-CreERT2.ENG*fl/fl* mice received one intraperitoneal injection with 10 mg/mL azoxymethane (AOM; Sigma-Aldrich, Zwijndrecht, The Netherlands) dissolved in saline. Two days later, the first 7-day cycle with 1.5% dextran sodium sulphate (DSS; MP Biomedicals, Santa Ana, CA, USA) dissolved in drinking water, supplemented with artificial sweetener (Natrena), was started. After seven days, drinking water was changed to standard conditions for 14 days. This three-week cycle was repeated twice more during the experiment. During DSS cycles mice weight and overall health were monitored daily, while during the "off" period animals were weighted and checked every other day. Two weeks after the third DSS cycle, mice were sacrificed and blood and tissue samples were collected. Colons were fixed in 4% formaldehyde and photographed. Lesion volume was measured in photographed colons by ImageJ (National Institute of Health) and tumor volume was calculated (tumor volume = (width^2 × length)/2).

RT-qPCR

Tissue samples were disintegrated using a TissueLyser (Qiagen, Hilden, Germany) and RNA was isolated using Nucleospin RNA kit (Bioké, Leiden, The Netherlands), according to manufacturers' instructions. For *in vitro* experiments, MEFs were grown to confluency, harvested and RNA was isolated as described above. RNA concentration and purity were determined using NanoDrop 3300 (Thermo Scientific, Breda, The Netherlands). Complementary DNA synthesis was performed using 1 μg RNA using RevertAid First Strand cDNA synthesis kit, according to manufacturers' instructions (ThermoScientific).

Quantitative PCR analyses were performed as described before (*8*), using primers as described in supplementary table S1 (Invitrogen). All values were normalized by *GAPDH* expression.

Fluorescence-activated cell sorting

Tumor material was minced with scalpels and digested with Liberase (Roche, Basel, Switzerland) according to manufacturer's protocol. Single cell suspensions were made and stained with antibodies against CD45, CD11b (both eBioscience, Vienna, Austria), F4/80, Ly6C and Ly6G (all BioLegend, San Diego, CA, USA). FACS analysis was performed on a LSR II system (Becton Dickinson, Breda, The Netherlands). Data was analyzed using FlowJo data analysis software (FlowJo, Ashland, OR, USA).

Tissue analysis

Immunohistochemical stainings were performed as described previously (*39*), using primary antibodies against vimentin, cleaved caspase 3 (both Cell Signaling Technologies, Danvers, MA, USA), αSMA (Progen, Heidelberg, Germany), Ki67 (Millipore, Amsterdam, The Netherlands), Ly6G (BioLegend), F4/80 (eBioscience) and endoglin (R&D systems, Abington, UK). For quantification of total collagen, tumor sections were stained with Sirius red (Klinipath, Duiven, The Netherlands). In short, paraffin sections were deparaffinized, stained with 0.1% Sirius red in picric acid, washed in 0.01M HCl and subsequently dehydrated and mounted in entellan. Three to five representative pictures per mouse were taken with an Olympus BX51TF microscope (Olympus Life Science Solutions, Zoeterwoude, The Netherlands) and staining was quantified using ImageJ software (National Institutes of Health). Quantification of macrophage infiltration was scored based on F4/80 staining. Score 1; ≤5% stroma positive, score 2; 5-25% stroma positive, score 3; 25-50% stroma positive, score 4; ≥50% stroma positive.

Statistical analysis

Tissue analysis was performed in a blinded manner by two independent observers. Data indicate mean ± s.e.m. or SD, as indicated in figure legends. Differences between groups were calculated using Students' *t*-test or Mann-Whitney analysis. P-values ≤0.05 were considered statistical significant.

Results

Fibroblast-specific endoglin knock out enhances AOM/DSS-induced adenoma formation

In order to assess the effect of inducible collagen1α1-specific endoglin deletion on AOM/DSS-induced tumor formation, collagen1α1-Cre-ERT2 mice were crossbred with ENG*fl/fl* mice, generating collagen1α1-CreERT2.ENG*fl/fl* mice. Cre-mediated recombination

was induced in 8-week old animals by oral administration of tamoxifen, generating ENG$^{Fib-/-}$ mice. Animals were exposed to the AOM/DSS protocol as described in figure 1A. Throughout the course of the experiment, mice in both groups showed weight loss during DSS supplementation, which recovered during the "off" periods (Supplementary fig. S1A). Upon termination of the experiment, the number of lesions in the colorectum was quantified. The occurrence of colonic lesions was strongly increased in the ENG$^{Fib-/-}$ group when compared with control mice (Fig. 1B and C). Although the number of tumors differed, average lesion size was similar in both groups (Fig. 1D). In the ENG$^{Fib-/-}$ group serious complications, including rectal blood loss, rectal prolapse or substantial weight loss, were more often observed, reflecting the more severe phenotype resulting in premature animal sacrifice. The number of lesions per mouse was not dependent on sex of the animals (Supplementary fig. S1B). Lesions were analyzed by H&E staining and characterized by a pathologist as adenomas with high grade dysplasia (Fig. 1E). Throughout the course of our experiments, no neoplastic growth at other locations than the colorectum was observed. These data suggest that endoglin on fibroblasts plays an important role in chemically-induced colorectal tumorigenesis.

Fibroblast-specific endoglin knock out does not induce spontaneous adenoma formation

To exclude that endoglin deletion in fibroblasts results in spontaneous neoplastic growth, collagen1α1-CreERT2.ENG*fl/fl* mice were induced with tamoxifen. Animals were housed for 13 weeks, identical to the time course of the experiment, and were not treated with AOM or DSS. At the end of the experiment lesion formation in the colorectum was assessed. In both ENG$^{Fib-/-}$ and control mice, no lesions in the colorectum were observed (Supplementary fig. S1C). Additional histological analysis did not reveal any morphological changes in the colon (data not shown). This suggests that fibroblast-specific endoglin knock out does not result in spontaneous neoplastic growth during the course of our experiments.

Additionally, to assess the effect of tamoxifen administration on tumor induction, ENG*fl/fl* mice without the Cre recombinase, as a negative control, received oral tamoxifen and were subsequently exposed to the AOM/DSS regimen as described in figure 1A. After 13 weeks, the number of lesions in the colorectum of tamoxifen-induced ENG*fl/fl* mice was similar to non-induced Collagen1α1-CreERT2.ENG*fl/fl* mice treated with AOM and DSS (Supplementary fig. S1C). This implies that tamoxifen administration does not affect AOM/DSS-induced lesion formation in our model.

Fibroblast-specific endoglin knock out increases stromal content

Disturbance of paracrine signaling between stromal and epithelial cells can result in increased proliferation or decreased apoptosis rates, thereby contributing to tumor formation. Therefore, we analyzed adenomas from control and ENG$^{Fib-/-}$ mice to assess changes in these processes. First, we determined the proliferation rate in AOM/DSS-induced lesions using Ki67 expression, the cellular marker for proliferation, by immunohistochemistry

and quantified the number of Ki67 positive cells. Upon quantification, similar numbers of proliferating cells were observed in both groups (Fig. 2A). Next, we stained for the apoptotic marker cleaved caspase 3 and counted the number of apoptotic cells in the adenomas. The number of apoptotic cells was similar in both control and ENG$^{Fib-/-}$ mice (Fig. 2B).

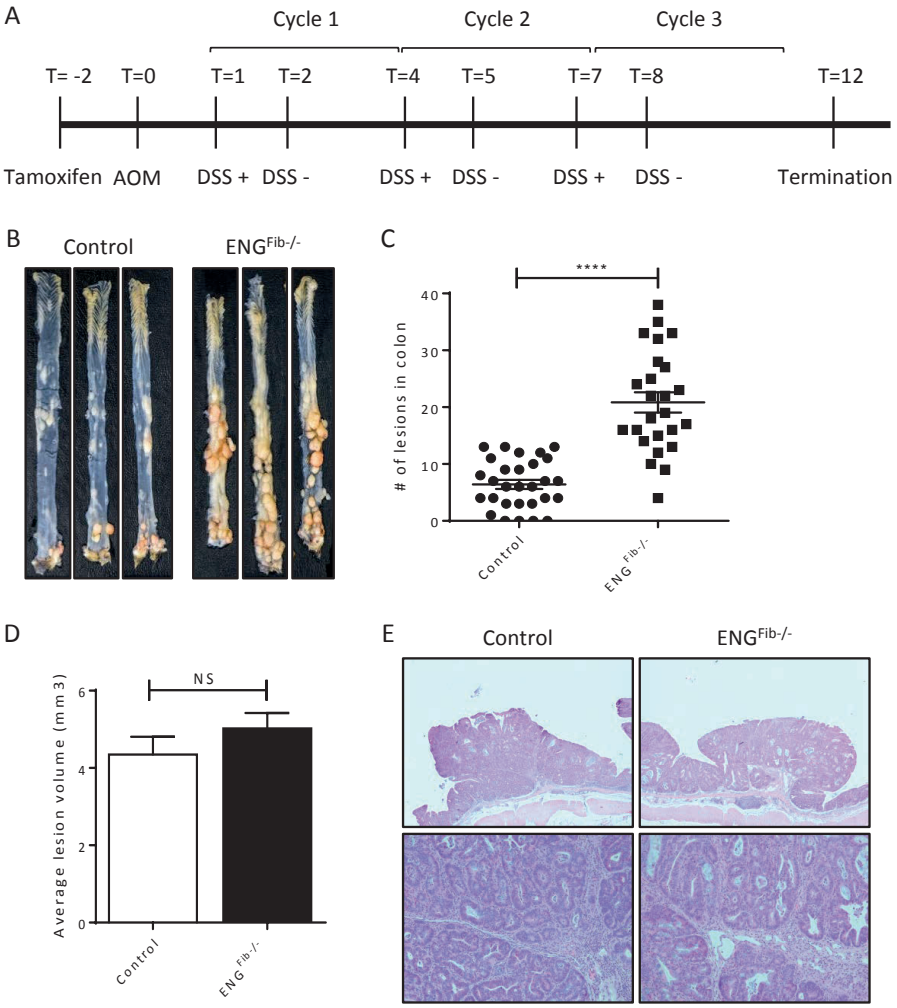

Figure 1. Fibroblast-specific endoglin knock out enhances AOM/DSS-induced neoplastic growth. A. Experimental set-up. At 8 weeks of age, mice were induced with tamoxifen. After two weeks, AOM was injected, followed by three 21-day DSS cycles. Two weeks after the last DSS cycle, experiments were terminated. B. Representative pictures of colons obtained from control and fibroblast-specific endoglin knock out (ENG$^{Fib-/-}$) mice at end of the experiment. C. Neoplastic growth was highly increased in ENG$^{Fib-/-}$ mice, although size of the lesions did not differ between the groups (D). E. Histological analysis of AOM/DSS-induced lesions revealed adenomas with high grade dysplasia. Graphs represent mean of 29-25 mice/group from two independent experiments. ****P≤0.0001.

Since fibroblasts are the major component of the tumor stroma, the effect of fibroblast-specific endoglin deletion on total stroma content of the lesions was assessed by vimentin staining. Lesions from $ENG^{Fib-/-}$ mice showed a significant increase in vimentin positive cells, when compared with control mice (Fig. 2C). Next, αSMA staining was used to determine the proportion of activated fibroblasts in the stroma. As observed for vimentin, the percentage of αSMA-positive content was increased in $ENG^{Fib-/-}$ lesions compared with the control (Fig. 2D). Although more αSMA-positive fibroblasts were observed in $ENG^{Fib-/-}$ lesions, total collagen production as determined using Sirius red staining, did not differ between the two groups (Fig. 2E). Together, these data imply that, without affecting the balance between proliferation and apoptosis in intestinal epithelium, expansion of the stromal compartment might contribute to neoplastic growth in our model.

Enhanced immune infiltration in fibroblast-specific endoglin knock out adenomas

Cancer-associated fibroblasts have been shown to secrete chemoattractants and hereby regulate recruitment of immune cells to the tumor (*12*). Moreover, immune cells are proven to be an important part of the tumor microenvironment and promote tumor initiation and progression (*40-43*). Therefore, we determined the extent and composition of immune infiltrate in the AOM/DSS-induced lesions. Upon termination of the experiment, neoplastic tissues of three mice per group were subjected to flow cytometry. Total immune infiltrate, based on CD45 expression, was not significantly changed between the control and $ENG^{Fib-/-}$ group (Fig.3A). However, when we determined the percentage CD11b-expressing cells (monocytes and macrophages) in the CD45+ population, increased infiltration was observed in $ENG^{Fib-/-}$ lesions (Fig.3B). In order to further specify this CD11b+ population, the abundance of macrophages was determined using Ly6C expression. Although Ly6C+ monocytes appeared to be increased in the $ENG^{Fib-/-}$ group, this did not reach statistical significance (Fig.3C). The percentage of Ly6C- macrophages, though, was significantly increased in $ENG^{Fib-/-}$ lesions, when compared with controls (Fig.3D). Increased macrophage recruitment to $ENG^{Fib-/-}$ lesions was confirmed by quantification of immunohistochemical staining for the macrophage marker F4/80 (Fig.3E).

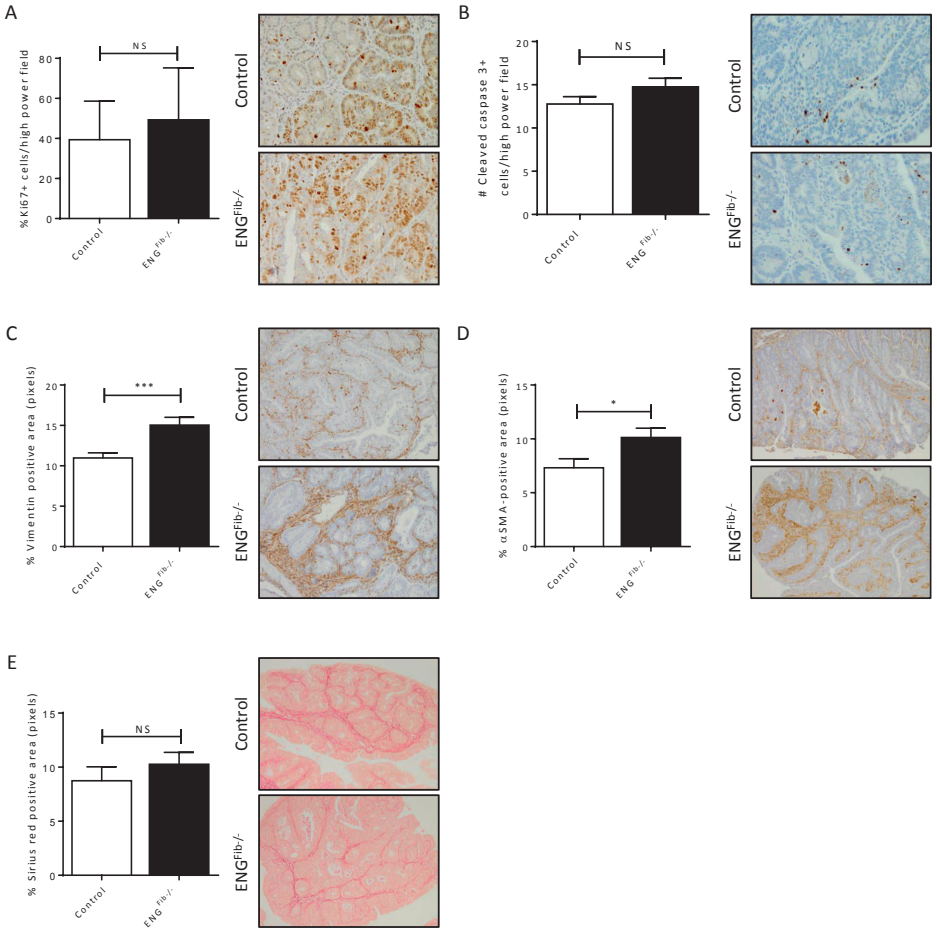

Figure 2. Endoglin deletion in fibroblasts increases stromal component in AOM/DSS-induced lesions. A. Cellular proliferation in tumors was assessed by Ki67 staining and was similar in the control and ENG$^{Fib-/-}$ group. B. Apoptosis was determined by cleaved caspase 3 staining, which did not show a difference between the two groups. C. Total stroma content as quantified by vimentin staining and the abundance of activated fibroblasts as assessed by αSMA staining (D), proved to be increased after fibroblast-specific endoglin deletion. E. Total collagen deposition as measure by Sirius red was not affected by endoglin knock out in fibroblasts. Data represent 24/23 mice per group from two independent experiments, average number of positive pixels or average number of cells per high power field. *P≤0.05, ***P≤0.001.

Additionally, we assessed neutrophil infiltration in tumors using Ly6G expression. Flow cytometry showed that the percentage of Ly6G+ cells in the CD45+ population was strongly increased in the ENG$^{Fib-/-}$ group, when compared with control mice (Fig.4A). The number of Ly6G+ cells in adenomas was also assessed by IHC, and this analysis confirmed higher neutrophil infiltrate upon fibroblast-specific endoglin knock out (Fig. 4B). These data suggest that fibroblast-specific deletion of endoglin results in enhanced recruitment of immune cells, mainly macrophages and neutrophils.

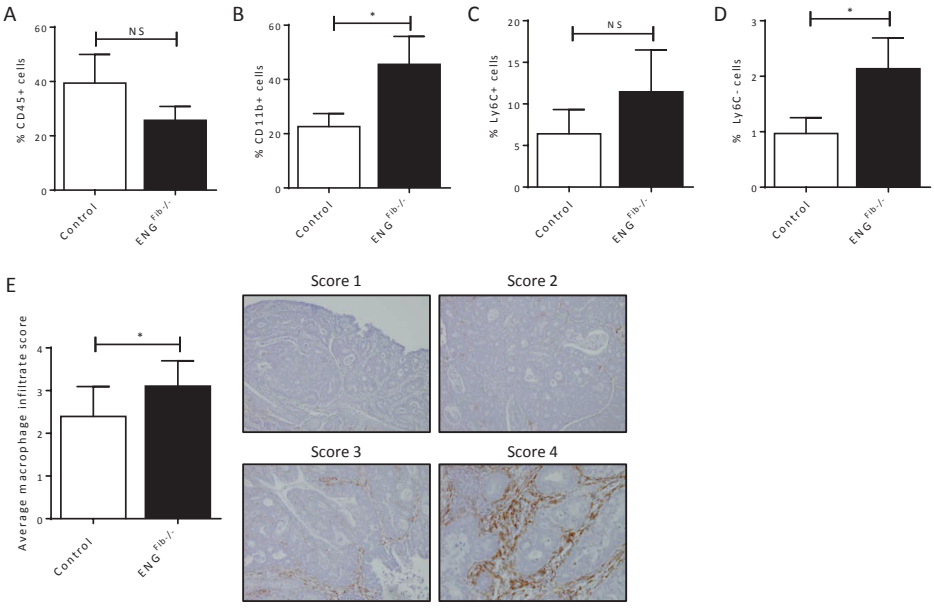

Figure 3. Increased macrophage recruitment to ENG$^{Fib-/-}$ lesions. Immune cell infiltrate in the lesions was determined using flow cytometry. CD45+ cells were gated out of the life cell population (A). Subsequently, CD11b+ cells were gated out of CD45+ (B). Next, F4/80 expressing cells were selected from the CD11b+ population. Using Ly6C expression, subdivision between Ly6C+ monocytes (C) and Ly6C- macrophages (D) was made, showing increased macrophage infiltration in ENG$^{Fib-/-}$ lesions. (n=3 tumors/group) E. The extent of macrophage infiltration was scored based on F4/80 IHC. Score 1; ≤5% stroma positive, score 2; 5-25% stroma positive, score 3; 25-50% stroma positive, score 4; ≥50% stroma positive. (n= 11-12 tumors/group). *P≤0.05.

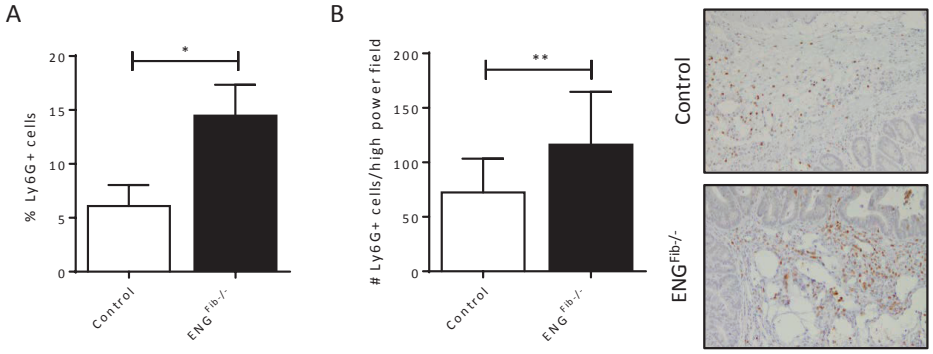

Figure 4. Fibroblast-specific endoglin deletion increases neutrophil recruitment. A. Flow cytometry showed increased neutrophil infiltrate in ENG$^{Fib-/-}$ lesions. Neutrophils were selected by gating for Ly6G from the CD45+/CD11b+ population. (n=3 tumors/group) B. IHC for Ly6G confirmed increased neutrophil influx in ENG$^{Fib-/-}$ lesions. Graph represents 24/23 mice per group from two independent experiments, average number of Ly6G+ cells. *P≤0.05, **P≤0.01.

Endoglin knock out in MEFs affects expression of inflammation-related genes *in vitro*

In order to confirm our *in vivo* observations that endoglin deletion in fibroblasts does not lead to increased epithelial proliferation in AOM/DSS induced lesions, *in vitro* proliferation was assessed. Since shRNA-mediated knockdown of endoglin in fibroblasts results in a lethal phenotype *in vitro* (chapter 7), we made use of murine embryonic fibroblasts (MEFs) from ENG*fl/fl* mice. Using lentiviral transduction, Cre recombinase was introduced in these cells, resulting in genetic deletion of endoglin (Fig. 5A). Conditioned medium (CM) from empty vector and endoglin knock out MEFs was prepared to assess paracrine signaling to mouse epithelial cells. CT26 and MC38 mouse CRC cells were stimulated with CM from either empty vector control or endoglin knock out MEFs and proliferation was measured. Over the course of three days, proliferation rates between non-stimulated cells, control CM or endoglin knock out CM stimulated cells were similar in both CT26 (Fig. 5B) and MC38 cells (Fig. 5C). This suggests that endoglin on fibroblasts does not directly affect epithelial tumor cell proliferation by secreting paracrine factors *in vitro,* confirming our *in vivo* findings. When we stimulated MC38 CRC cells with CM and assessed BMP signaling using the Bre-Luc reporter construct, response to control and endoglin knock out CM was similar and did not induce BMP signaling (Fig. 5D). Since MC38 cells were not responsive to TGF-β stimulation, we have used the mouse myoblast cell line C2C12 to determine effects of MEF CM on TGF-β signaling. Preliminary data show that TGF-β signaling was significantly induced by TGF-β stimulation and CM from control MEFs, whereas CM from endoglin knock out MEFs did not induce a response (Fig. 5E).

Next, considering the role of fibroblasts in immune cell recruitment by secretion of immunomodulatory factors, we assessed gene expression of these factors after endoglin knock out in MEFs. For this, RT-qPCR analysis was performed on empty vector control and endoglin knock out MEFs. Endoglin knock out in MEFs resulted in upregulation of IL-7 and MMP-9 (Fig. 6A) and downregulation of IL-8, TNFα, CXCR2, BMP-6, CXCL1 and all isoforms of TGF-β (Fig.6B). These data show that endoglin knock out in fibroblasts affects expression of TGF-β/BMP ligands and immunoregulatory factors.

Fibroblast-specific endoglin knock out changes immunoregulatory expression profiles *in vivo*

Based on the increased immune filtration in the lesions and differential expression of immunomodulatory factors in MEFs, we next assessed gene expression profiles of immune modulators in AOM/DSS-induced adenomas. As expected, endoglin expression was lower in lesions obtained from $ENG^{Fib-/-}$ mice, when compared with controls (Fig.7A). Additionally, as observed in MEFs, BMP-6 was expressed at lower levels in $ENG^{Fib-/-}$ lesions (Fig.7A). Although not significantly changed, we observed downregulation of CCL2, IL-2 and IL-7 in $ENG^{Fib-/-}$ lesions (Fig. 7B). Furthermore, mRNA expression of IL-6, IL-10, PDGFβ, IFNγ and SDF-1 was also decreased upon fibroblast-specific endoglin deletion (Fig. 7B). Moreover,

upregulation of the neutrophil attractant CXCL2 was observed in lesions from ENG$^{Fib-/-}$ mice (Fig. 7C), which is in agreement with increased neutrophil influx. Combined, these data show that fibroblast-specific endoglin deletion changes gene expression profiles of immunoregulatory genes *in vivo*.

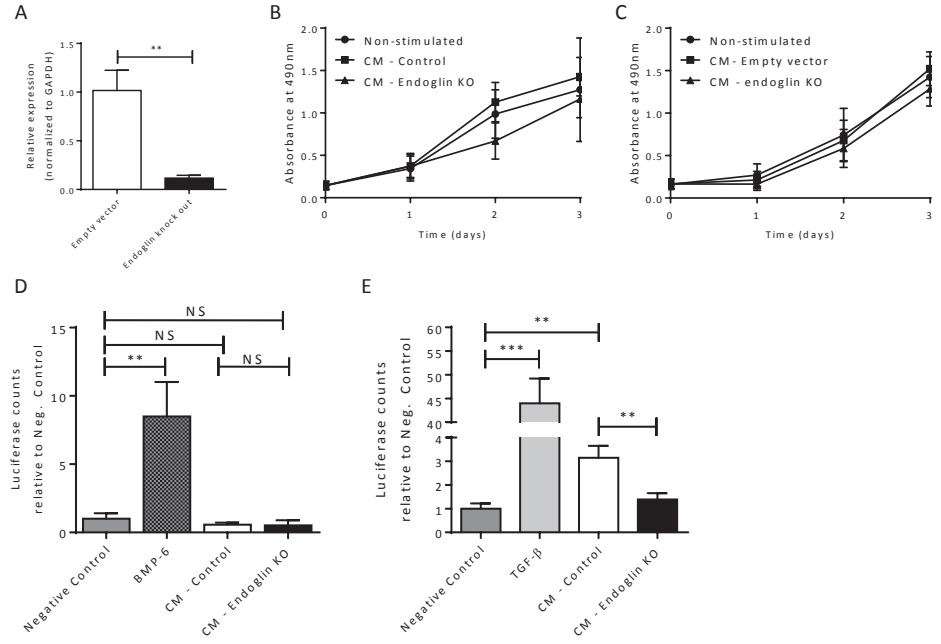

Figure 5. Conditioned medium from endoglin knock out MEFs lacks TGF-β-activating paracrine factors. A. MEFs were transduced with a Cre expressing lentivirus or empty vector control, significantly reducing endoglin expression after transduction with Cre recombinase. Graph represents mean of three independent experiments. Stimulation with conditioned medium from MEFs, either empty vector (CM – Control) or endoglin knock out (CM – Endoglin KO), did not affect tumor cell proliferation in CT26 (B) or MC38 cells (C). Graphs represent mean of three independent experiments performed in triplicate. D. Stimulation with CM from either empty vector or endoglin knock out MEFs did not enhance BMP signaling in a luciferase reporter assay. Graph represents mean of three experiments, performed in triplicate. E. TGF-β signaling was determined using the CAGA-Luc reporter construct, showing that CM from control MEFs induced TGF-β signaling in C2C12 cells, whereas CM from endoglin knock out MEFs did not. Graph represents single experiment, performed in triplicate. **P≤0.01, ***P≤0.001.

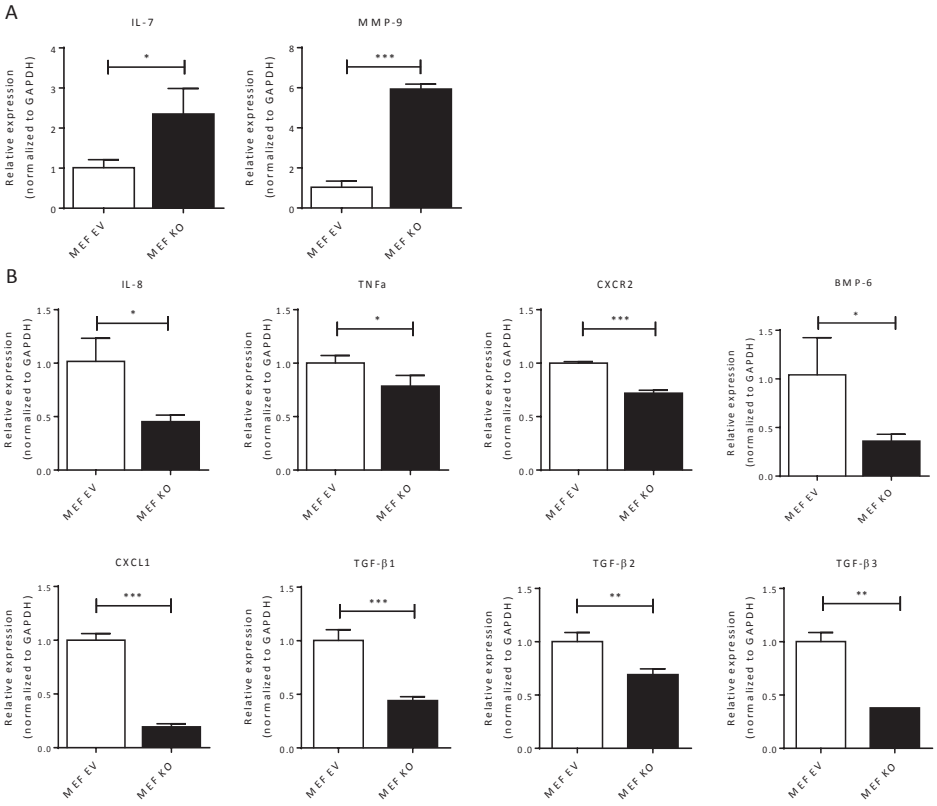

Figure 6. Endoglin knock out changes expression of chemokines in MEFs. RT-qPCR was performed to assess expression patterns of immunoregulatory genes. Endoglin knock out resulted in increased IL-7 and MMP-9 expression (A), while mRNA levels of IL-8, TNFα, CXCR2, BMP-6, CXLC1 and all TGF-β isoforms were decreased (E). Graphs represent data from three independent experiments. *P≤0.05, **P≤0.01, ***P≤0.001.

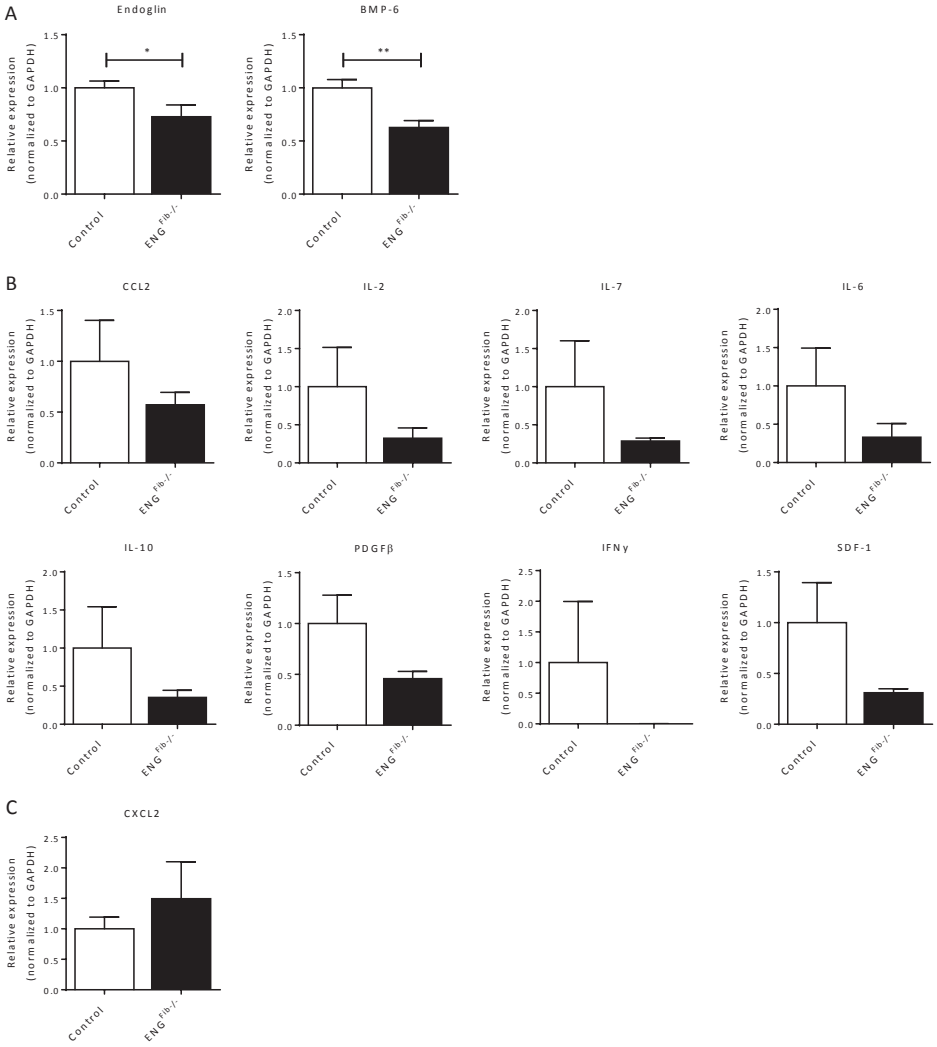

Figure 7. ENG$^{Fib-/-}$ lesions display changed expression of immunoregulatory genes. A. Lesions from ENG$^{Fib-/-}$ mice showed decreased expression of endoglin and BMP-6 at mRNA levels. B. A trend in decreased expression in the ENG$^{Fib-/-}$ group was observed for CCL2, IL-2, IL-7, IL-6, IL-10, PDGFβ, IFNγ and SDF-1. Expression of CXCL2 appeared to be increased (C). Graphs represent 9-5 lesions/group from two independent experiments. *P≤0.05, **P≤0.01.

Discussion

In this study we show that fibroblast-specific endoglin deletion increases tumorigenesis in a mouse model for inflammation-associated CRC. Fibroblast-specific endoglin deletion did not affect epithelial cell proliferation in adenomas, but resulted in stromal expansion and increased influx of macrophages and neutrophils into the lesions.

In intestinal homeostasis, the interplay between stroma and epithelium is crucial. When disrupted, imbalance in this interaction leads to decreased epithelial apoptosis or an increase in stem cell proliferation (*44, 45*), both resulting in spontaneous polyp formation. As shown by Beppu et al., inactivation of the BMP receptor type II (BMPRII) in intestinal stromal cells, increased epithelial cell proliferation and resulted in local polyp formation in the mouse colorectum (*46*). Similar effects have been observed for TGF-β receptor type II (TβRII) deletion in fibroblasts, resulting in neoplastic growth in the prostate and invasive stomach carcinoma *in vivo (47)*. Inactivation of BMPRII or TβRII leads to tumor formation within seven weeks in the colorectum or stomach, respectively (*46, 47*). In our study, we did not observe spontaneous tumor formation after endoglin deletion in fibroblasts during the 13-week experimental period. This observation is supported by our *in vitro* proliferation data, where stimulation with conditioned medium from endoglin knock out MEFs did not affect proliferation in two mouse CRC cell lines. These data suggest that endoglin expression on fibroblasts is not involved in regulating proliferation or apoptosis through paracrine factors.

Although no spontaneous tumors developed, fibroblast-specific endoglin deletion enhanced chemically-induced adenoma formation. One of the differences between lesions from the control and $ENG^{Fib-/-}$ group, was the increase of activated fibroblasts upon endoglin knock out. The $ENG^{Fib-/-}$ mice show worse survival due to complications of the high number of tumors. In CRC patients, the abundance of tumor stroma was reported to be prognostic for both overall and metastasis-free survival (*48*). This could imply that $ENG^{Fib-/-}$ lesions would be more aggressive and could have a higher metastatic potential. However, the severity of discomfort in our model does not allow for a prolonged experimental period, therefore tumor progression and metastatic spread could not be evaluated.

Contradictory to our observations reported here, our own recently published data show that treatment with the endoglin neutralizing antibody TRC105 reduced αSMA-positive tumor content in an *in vivo* breast cancer model (*49*). Additionally, a study in endoglin heterozygous mice reported that αSMA-positive content in prostate tumors was decreased, when compared to endoglin wild type mice (*50*). A major difference between aforementioned studies and our current research is that heterozygote endoglin deletion and TRC105 affect all cells expressing endoglin, which might explain the differential effects observed when compared to fibroblast-specific endoglin deletion.

In cancer, increased presence of activated fibroblasts in the stroma is known to regulate a TGF-β-induced fibrotic response, thereby stimulating tumor progression (*51, 52*). However, contradictory results have been published suggesting endoglin as either a

negative or a positive regulator of fibrosis (reviewed in (*53*)).The importance of endoglin in the fibrotic response was shown by decreased cardiac fibrosis in endoglin heterozygous mice (*54*). Moreover, in a mouse model for wound healing endoglin heterozygosity resulted in persistence of activated fibroblasts in wounds, which is related to fibrosis (*55*). This persistence could be an underlying mechanism for the increased presence of αSMA-positive cells in the $ENG^{Fib-/-}$ lesions in our study. Interestingly, during liver fibrosis, both cellular expression of endoglin and plasma levels of soluble endoglin, cleaved from the membrane by MMP-14 (*56*), are increased. These levels are even further enhanced in patients with both hepatocellular carcinoma (HCC) and liver cirrhosis, implying a role for endoglin in fibrosis-mediated disease progression (*57*). However, in our experiments total collagen deposition, as a marker for fibrosis, was similar in both groups. Yet, fibrosis is a highly TGF-β-dependent process (*58*). Therefore, the decreased expression of TGF-β after endoglin knock out (Fig. 6B) might partly explain the unaffected levels of collagen deposition in AOM/DSS-induced lesions.

Besides directly stimulating tumor progression, CAFs also produce cytokines and chemokines which can regulate the influx of immune cells. Immune cells can either inhibit or enhance tumor progression and metastasis (*59*). Heterozygous expression of endoglin has been shown to result in progression of acute inflammation to chronic inflammation after a single high dose of DSS, whereas in wild type mice inflammation was resolved after two weeks (*60*). Increased expression of vascular endothelial growth factor (VEGF) in endoglin heterozygous mice was proposed to be responsible for the persistent inflammation. Both *in vitro* and in AOM/DSS-induced adenomas, we did not observe a significant change in VEGF expression after endoglin knock out (Supplementary fig.S2). This discrepancy might be caused by the specific deletion of endoglin in fibroblasts, excluding other endoglin-positive VEGF producing cells, like endothelial cells.

Macrophages were shown to be one of the immune cells that have tumor promoting effects by, amongst others, releasing growth factors and proteases (*61-63*). Dependent on macrophage subset, these cells can be either tumor-promoting or -suppressive (*61, 64*). Infiltration of macrophages is generally correlated to worse prognosis in various types of cancer (*65-71*). However, in CRC high macrophage infiltration has been shown to correlate with a better prognosis, although macrophage subsets also play a differential role in this type of cancer (*72-76*). In our model, the ratio of M1/M2 macrophages could be informative regarding changed macrophage abundance in $ENG^{Fib-/-}$ adenomas and should therefore be assessed in future experiments.

Based on flow cytometry and IHC, we also observed increased neutrophil infiltration in lesions from $ENG^{Fib-/-}$ mice. Tumor promoting and pro-metastatic roles were reported for neutrophils, mainly via protease activation and secretion of pro-angiogenic factors (*77-81*). Moreover, neutrophils were shown to play a crucial role in AOM/DSS-induced tumorigenesis, since neutrophil depletion resulted in significantly reduced tumor initiation (*82, 83*). We observed a trend to increased CXCL2 expression in lesions from $ENG^{Fib-/-}$ mice, which is a

neutrophil attracting chemokine that is highly expressed by tumor stroma (*83*), thereby explaining increased neutrophil recruitment. Additionally, decreased IL-6 levels, as seen in tumors from ENG$^{Fib-/-}$ mice, were shown to result in increased neutrophil recruitment (*84*), posing another explanation for increased neutrophil infiltration. Both CXCL2 and IL-6 are highly produced by CAFs in CRC (*14*). Our data suggest opposite regulatory mechanisms of endoglin on fibroblasts in CXCL2 and IL-6 expression. Therefore, endoglin deletion in fibroblasts could simultaneously increase neutrophil attracting and reduce neutrophil repellant cytokines, thereby increasing overall neutrophil recruitment, as observed in our study.

BMP-6 was the only factor which was significantly downregulated in both endoglin knock out MEFs and ENG$^{Fib-/-}$ lesions. High levels of BMP-6 were shown to inhibit proliferation of breast cancer and myeloma cells *in vitro (85-87)* and appear to reduce aggressiveness of breast cancer cells in a zebrafish model (*88*). Lower levels of BMP-6 could therefore relieve inhibitory effects on epithelial cell proliferation and enhance tumor growth. However, since we did not observed effects on epithelial proliferation, BMP-6 does not seem to regulate neoplastic growth in our model.
Furthermore, BMP-6 reduces macrophage proliferation (*89*), suggesting that the decreased levels of BMP-6 in ENG$^{Fib-/-}$ lesions could release inhibition of macrophage proliferation, thereby posing an explanation for the increased presence of macrophages. However, mRNA levels do not directly reflect BMP-6 protein and activity levels, of which the latter is regulated by proteolytic cleavage (*90*), complicating definitive conclusions based on mRNA expression.
In summary, we show here that fibroblast-specific endoglin knock out results in enhanced initiation of neoplastic growth in a chemically-induced model for CRC. Based on our results we suggest that fibroblast-specific endoglin deletion results in changed expression profiles of immunoregulatory factors, thereby leading to increased immune cell recruitment and enhanced tumorigenesis. More specifically, due to the crucial role of neutrophils in AOM/DSS-induced tumors, we propose that increased neutrophil recruitment in ENG$^{Fib-/-}$ mice greatly contributes to chemically-induced neoplastic growth. To confirm that endoglin deletion in fibroblasts results in increased neutrophil-mediated tumorigenesis, experiments in ENG$^{Fib-/-}$ mice, in the context of neutrophil depletion should be performed.

Acknowledgements

This study was supported by the Alpe d'HuZes/ Bas Mulder award 2011 (UL2011-5051) to LH and MP. We thank Kirsten Lodder (Dept. Molecular Cell Biology, LUMC) and Marij Mieremet (Dept. Gastroenterology-Hepatology, LUMC) for technical support and Kees Sier (Dept. Surgery, LUMC) for valuable discussions.

References

1. J. P. Heath, Epithelial cell migration in the intestine. *Cell Biol Int* **20**, 139-146 (1996).
2. C. S. Potten, Kinetics and possible regulation of crypt cell populations under normal and stress conditions. *Bull Cancer* **62**, 419-430 (1975).
3. R. G. Vries, M. Huch, H. Clevers, Stem cells and cancer of the stomach and intestine. *Mol Oncol* **4**, 373-384 (2010).
4. A. P. Haramis *et al.*, De novo crypt formation and juvenile polyposis on BMP inhibition in mouse intestine. *Science* **303**, 1684-1686 (2004).
5. J. C. Hardwick *et al.*, Bone morphogenetic protein 2 is expressed by, and acts upon, mature epithelial cells in the colon. *Gastroenterology* **126**, 111-121 (2004).
6. E. Sancho, E. Batlle, H. Clevers, Signaling pathways in intestinal development and cancer. *Annu Rev Cell Dev Biol* **20**, 695-723 (2004).
7. M. Herrera *et al.*, Functional heterogeneity of cancer-associated fibroblasts from human colon tumors shows specific prognostic gene expression signature. *Clin. Cancer Res* **19**, 5914-5926 (2013).
8. L. J. Hawinkels *et al.*, Interaction with colon cancer cells hyperactivates TGF-beta signaling in cancer-associated fibroblasts. *Oncogene* **33**, 97-107 (2014).
9. P. Nyberg, T. Salo, R. Kalluri, Tumor microenvironment and angiogenesis. *Front Biosci* **13**, 6537-6553 (2008).
10. M. Van Bockstal *et al.*, Differential regulation of extracellular matrix protein expression in carcinoma-associated fibroblasts by TGF-beta1 regulates cancer cell spreading but not adhesion. *Oncoscience* **1**, 634-648 (2014).
11. W. G. Stetler-Stevenson, L. A. Liotta, D. E. Kleiner, Jr., Extracellular matrix 6: role of matrix metalloproteinases in tumor invasion and metastasis. *FASEB J* **7**, 1434-1441 (1993).
12. D. T. Fearon, The carcinoma-associated fibroblast expressing fibroblast activation protein and escape from immune surveillance. *Cancer Immunol. Res* **2**, 187-193 (2014).
13. M. L. Henriksson *et al.*, Colorectal cancer cells activate adjacent fibroblasts resulting in FGF1/FGFR3 signaling and increased invasion. *Am J Pathol* **178**, 1387-1394 (2011).
14. J. Tommelein *et al.*, Cancer-associated fibroblasts connect metastasis-promoting communication in colorectal cancer. *Front Oncol* **5**, 63 (2015).
15. L. Ronnov-Jessen, O. W. Petersen, V. E. Koteliansky, M. J. Bissell, The origin of the myofibroblasts in breast cancer. Recapitulation of tumor environment in culture unravels diversity and implicates converted fibroblasts and recruited smooth muscle cells. *J Clin Invest* **95**, 859-873 (1995).
16. M. P. Lewis *et al.*, Tumour-derived TGF-beta1 modulates myofibroblast differentiation and promotes HGF/SF-dependent invasion of squamous carcinoma cells. *Br J Cancer* **90**, 822-832 (2004).
17. D. Y. Li *et al.*, Defective angiogenesis in mice lacking endoglin. *Science* **284**, 1534-1537 (1999).
18. R. L. Carvalho *et al.*, Defective paracrine signalling by TGFbeta in yolk sac vasculature of endoglin mutant mice: a paradigm for hereditary haemorrhagic telangiectasia. *Development* **131**, 6237-6247 (2004).
19. H. M. Arthur *et al.*, Endoglin, an ancillary TGFbeta receptor, is required for extraembryonic angiogenesis and plays a key role in heart development. *Dev. Biol* **217**, 42-53 (2000).
20. F. Lebrin *et al.*, Endoglin promotes endothelial cell proliferation and TGF-beta/ALK1 signal transduction. *EMBO J* **23**, 4018-4028 (2004).
21. O. Nolan-Stevaux *et al.*, Endoglin Requirement for BMP9 Signaling in Endothelial Cells Reveals New Mechanism of Action for Selective Anti-Endoglin Antibodies. *PLoS. One* **7**, e50920 (2012).
22. H. Tian, K. Mythreye, C. Golzio, N. Katsanis, G. C. Blobe, Endoglin mediates fibronectin/alpha5beta1 integrin and TGF-beta pathway crosstalk in endothelial cells. *EMBO J* **31**, 3885-3900 (2012).
23. M. J. Goumans *et al.*, Activin receptor-like kinase (ALK)1 is an antagonistic mediator of lateral TGFbeta/ALK5 signaling. *Mol. Cell* **12**, 817-828 (2003).
24. M. J. Goumans *et al.*, Balancing the activation state of the endothelium via two distinct TGF-beta type I receptors. *EMBO J* **21**, 1743-1753 (2002).
25. P. ten Dijke, M. J. Goumans, E. Pardali, Endoglin in angiogenesis and vascular diseases. *Angiogenesis* **11**, 79-89 (2008).

26. T. Tanaka *et al.*, A novel inflammation-related mouse colon carcinogenesis model induced by azoxymethane and dextran sodium sulfate. *Cancer Sci* **94**, 965-973 (2003).
27. C. Neufert, C. Becker, M. F. Neurath, An inducible mouse model of colon carcinogenesis for the analysis of sporadic and inflammation-driven tumor progression. *Nat. Protoc* **2**, 1998-2004 (2007).
28. T. H. Corbett, D. P. Griswold, Jr., B. J. Roberts, J. C. Peckham, F. M. Schabel, Jr., Tumor induction relationships in development of transplantable cancers of the colon in mice for chemotherapy assays, with a note on carcinogen structure. *Cancer Res* **35**, 2434-2439 (1975).
29. M. G. Brattain, J. Strobel-Stevens, D. Fine, M. Webb, A. M. Sarrif, Establishment of mouse colonic carcinoma cell lines with different metastatic properties. *Cancer Res* **40**, 2142-2146 (1980).
30. J. Larsson *et al.*, Abnormal angiogenesis but intact hematopoietic potential in TGF-beta type I receptor-deficient mice. *EMBO J* **20**, 1663-1673 (2001).
31. K. R. Allinson, R. L. Carvalho, S. van den Brink, C. L. Mummery, H. M. Arthur, Generation of a floxed allele of the mouse Endoglin gene. *Genesis* **45**, 391-395 (2007).
32. O. Korchynskyi, P. ten Dijke, Identification and functional characterization of distinct critically important bone morphogenetic protein-specific response elements in the Id1 promoter. *J Biol Chem* **277**, 4883-4891 (2002).
33. U. Persson *et al.*, The L45 loop in type I receptors for TGF-beta family members is a critical determinant in specifying Smad isoform activation. *FEBS Lett* **434**, 83-87 (1998).
34. J. E. Kim, K. Nakashima, B. de Crombrugghe, Transgenic mice expressing a ligand-inducible cre recombinase in osteoblasts and odontoblasts: a new tool to examine physiology and disease of postnatal bone and tooth. *Am J Pathol* **165**, 1875-1882 (2004).
35. D. J. Liska, M. J. Reed, E. H. Sage, P. Bornstein, Cell-specific expression of alpha 1(I) collagen-hGH minigenes in transgenic mice. *J Cell Biol* **125**, 695-704 (1994).
36. A. R. Agarwal, R. H. Goldstein, E. Lucey, H. Q. Ngo, B. D. Smith, Cell-specific expression of the alpha 1 (I) collagen promoter-CAT transgene in skin and lung: a response to TGF-beta subcutaneous injection and bleomycin endotracheal instillation. *J Cell Biochem* **63**, 135-148 (1996).
37. E. Vuorio, B. de Crombrugghe, The family of collagen genes. *Annu Rev Biochem* **59**, 837-872 (1990).
38. N. M. Thoua *et al.*, Gut fibrosis with altered colonic contractility in a mouse model of scleroderma. *Rheumatology (Oxford)* **51**, 1989-1998 (2012).
39. L. J. Hawinkels *et al.*, Tissue level, activation and cellular localisation of TGF-beta1 and association with survival in gastric cancer patients. *Br. J. Cancer* **97**, 398-404 (2007).
40. S. Ostrand-Rosenberg, Immune surveillance: a balance between protumor and antitumor immunity. *Curr Opin Genet Dev* **18**, 11-18 (2008).
41. M. Karin, T. Lawrence, V. Nizet, Innate immunity gone awry: linking microbial infections to chronic inflammation and cancer. *Cell* **124**, 823-835 (2006).
42. K. E. de Visser, A. Eichten, L. M. Coussens, Paradoxical roles of the immune system during cancer development. *Nat Rev Cancer* **6**, 24-37 (2006).
43. F. Balkwill, K. A. Charles, A. Mantovani, Smoldering and polarized inflammation in the initiation and promotion of malignant disease. *Cancer Cell* **7**, 211-217 (2005).
44. L. E. Batts, D. B. Polk, R. N. Dubois, H. Kulessa, Bmp signaling is required for intestinal growth and morphogenesis. *Dev Dyn* **235**, 1563-1570 (2006).
45. D. Liu *et al.*, Dosage-dependent requirement of BMP type II receptor for maintenance of vascular integrity. *Blood* **110**, 1502-1510 (2007).
46. H. Beppu *et al.*, Stromal inactivation of BMPRII leads to colorectal epithelial overgrowth and polyp formation. *Oncogene* **27**, 1063-1070 (2008).
47. N. A. Bhowmick *et al.*, TGF-beta signaling in fibroblasts modulates the oncogenic potential of adjacent epithelia. *Science* **303**, 848-851 (2004).
48. W. E. Mesker *et al.*, The carcinoma-stromal ratio of colon carcinoma is an independent factor for survival compared to lymph node status and tumor stage. *Cell Oncol* **29**, 387-398 (2007).
49. M. Paauwe *et al.*, Endoglin targeting inhibits tumor angiogenesis and metastatic spread in breast cancer. *Oncogene*, (2016).
50. D. Romero *et al.*, Endoglin regulates cancer-stromal cell interactions in prostate tumors. *Cancer Res* **71**, 3482-3493 (2011).

51. M. H. Barcellos-Hoff, D. Lyden, T. C. Wang, The evolution of the cancer niche during multistage carcinogenesis. *Nat Rev Cancer* **13**, 511-518 (2013).
52. P. Cirri, P. Chiarugi, Cancer associated fibroblasts: the dark side of the coin. *Am. J. Cancer Res* **1**, 482-497 (2011).
53. J. A. Maring, M. Trojanowska, P. ten Dijke, Role of endoglin in fibrosis and scleroderma. *Int. Rev. Cell Mol. Biol* **297**, 295-308 (2012).
54. N. K. Kapur *et al.*, Reduced endoglin activity limits cardiac fibrosis and improves survival in heart failure. *Circulation* **125**, 2728-2738 (2012).
55. M. Pericacho *et al.*, Endoglin haploinsufficiency promotes fibroblast accumulation during wound healing through Akt activation. *PLoS. One* **8**, e54687 (2013).
56. L. J. Hawinkels *et al.*, Matrix metalloproteinase-14 (MT1-MMP)-mediated endoglin shedding inhibits tumor angiogenesis. *Cancer Res* **70**, 4141-4150 (2010).
57. E. Yagmur *et al.*, Elevation of endoglin (CD105) concentrations in serum of patients with liver cirrhosis and carcinoma. *Eur. J. Gastroenterol. Hepatol* **19**, 755-761 (2007).
58. M. Morikawa, R. Derynck, K. Miyazono, TGF-beta and the TGF-beta Family: Context-Dependent Roles in Cell and Tissue Physiology. *Cold Spring Harb Perspect Biol* **8**, (2016).
59. J. L. Markman, S. L. Shiao, Impact of the immune system and immunotherapy in colorectal cancer. *J Gastrointest Oncol* **6**, 208-223 (2015).
60. M. Jerkic *et al.*, Dextran sulfate sodium leads to chronic colitis and pathological angiogenesis in Endoglin heterozygous mice. *Inflamm Bowel Dis* **16**, 1859-1870 (2010).
61. S. K. Biswas, A. Mantovani, Macrophage plasticity and interaction with lymphocyte subsets: cancer as a paradigm. *Nat Immunol* **11**, 889-896 (2010).
62. A. Mantovani, S. Sozzani, M. Locati, P. Allavena, A. Sica, Macrophage polarization: tumor-associated macrophages as a paradigm for polarized M2 mononuclear phagocytes. *Trends Immunol* **23**, 549-555 (2002).
63. M. Erreni, A. Mantovani, P. Allavena, Tumor-associated Macrophages (TAM) and Inflammation in Colorectal Cancer. *Cancer Microenviron* **4**, 141-154 (2011).
64. C. Belgiovine, M. D'Incalci, P. Allavena, R. Frapolli, Tumor-associated macrophages and anti-tumor therapies: complex links. *Cell Mol Life Sci* **73**, 2411-2424 (2016).
65. T. O. Jensen *et al.*, Macrophage markers in serum and tumor have prognostic impact in American Joint Committee on Cancer stage I/II melanoma. *J Clin Oncol* **27**, 3330-3337 (2009).
66. T. Makitie, P. Summanen, A. Tarkkanen, T. Kivela, Tumor-infiltrating macrophages (CD68(+) cells) and prognosis in malignant uveal melanoma. *Invest Ophthalmol Vis Sci* **42**, 1414-1421 (2001).
67. R. D. Leek *et al.*, Association of macrophage infiltration with angiogenesis and prognosis in invasive breast carcinoma. *Cancer Res* **56**, 4625-4629 (1996).
68. S. Tsutsui *et al.*, Macrophage infiltration and its prognostic implications in breast cancer: the relationship with VEGF expression and microvessel density. *Oncol Rep* **14**, 425-431 (2005).
69. T. Hanada *et al.*, Prognostic value of tumor-associated macrophage count in human bladder cancer. *Int J Urol* **7**, 263-269 (2000).
70. I. Hamada *et al.*, Clinical effects of tumor-associated macrophages and dendritic cells on renal cell carcinoma. *Anticancer Res* **22**, 4281-4284 (2002).
71. C. Y. Chai *et al.*, Hypoxia-inducible factor-1alpha expression correlates with focal macrophage infiltration, angiogenesis and unfavourable prognosis in urothelial carcinoma. *J Clin Pathol* **61**, 658-664 (2008).
72. A. Algars *et al.*, Type and location of tumor-infiltrating macrophages and lymphatic vessels predict survival of colorectal cancer patients. *Int J Cancer* **131**, 864-873 (2012).
73. J. Forssell *et al.*, High macrophage infiltration along the tumor front correlates with improved survival in colon cancer. *Clin Cancer Res* **13**, 1472-1479 (2007).
74. C. Lackner *et al.*, Prognostic relevance of tumour-associated macrophages and von Willebrand factor-positive microvessels in colorectal cancer. *Virchows Arch* **445**, 160-167 (2004).
75. Q. Zhou *et al.*, The density of macrophages in the invasive front is inversely correlated to liver metastasis in colon cancer. *J Transl Med* **8**, 13 (2010).

76. S. Edin *et al.*, The distribution of macrophages with a M1 or M2 phenotype in relation to prognosis and the molecular characteristics of colorectal cancer. *PLoS One* **7**, e47045 (2012).
77. J. E. De Larco, B. R. Wuertz, L. T. Furcht, The potential role of neutrophils in promoting the metastatic phenotype of tumors releasing interleukin-8. *Clin Cancer Res* **10**, 4895-4900 (2004).
78. P. Scapini *et al.*, CXCL1/macrophage inflammatory protein-2-induced angiogenesis in vivo is mediated by neutrophil-derived vascular endothelial growth factor-A. *J Immunol* **172**, 5034-5040 (2004).
79. J. Jablonska, S. Leschner, K. Westphal, S. Lienenklaus, S. Weiss, Neutrophils responsive to endogenous IFN-beta regulate tumor angiogenesis and growth in a mouse tumor model. *J Clin Invest* **120**, 1151-1164 (2010).
80. M. M. Queen, R. E. Ryan, R. G. Holzer, C. R. Keller-Peck, C. L. Jorcyk, Breast cancer cells stimulate neutrophils to produce oncostatin M: potential implications for tumor progression. *Cancer Res* **65**, 8896-8904 (2005).
81. S. J. Huh, S. Liang, A. Sharma, C. Dong, G. P. Robertson, Transiently entrapped circulating tumor cells interact with neutrophils to facilitate lung metastasis development. *Cancer Res* **70**, 6071-6082 (2010).
82. K. Shang *et al.*, Crucial involvement of tumor-associated neutrophils in the regulation of chronic colitis-associated carcinogenesis in mice. *PLoS One* **7**, e51848 (2012).
83. T. Jamieson *et al.*, Inhibition of CXCR2 profoundly suppresses inflammation-driven and spontaneous tumorigenesis. *J Clin Invest* **122**, 3127-3144 (2012).
84. S. M. Hurst *et al.*, Il-6 and its soluble receptor orchestrate a temporal switch in the pattern of leukocyte recruitment seen during acute inflammation. *Immunity* **14**, 705-714 (2001).
85. W. J. Lian *et al.*, Downregulation of BMP6 enhances cell proliferation and chemoresistance via activation of the ERK signaling pathway in breast cancer. *Oncol Rep* **30**, 193-200 (2013).
86. F. Hu *et al.*, BMP-6 inhibits cell proliferation by targeting microRNA-192 in breast cancer. *Biochim Biophys Acta* **1832**, 2379-2390 (2013).
87. T. B. Ro *et al.*, Bone morphogenetic protein-5, -6 and -7 inhibit growth and induce apoptosis in human myeloma cells. *Oncogene* **23**, 3024-3032 (2004).
88. M. de Boeck *et al.*, Smad6 determines BMP-regulated invasive behaviour of breast cancer cells in a zebrafish xenograft model. *Sci Rep* **6**, 24968 (2016).
89. J. H. Hong *et al.*, Effect of bone morphogenetic protein-6 on macrophages. *Immunology* **128**, e442-450 (2009).
90. B. Bragdon *et al.*, Bone morphogenetic proteins: a critical review. *Cell Signal* **23**, 609-620 (2011).

Supplementary data

Supplementary table S1 Primer sequences as used for RT-qPCR analysis

Gene	Forward	Reverse
GAPDH	AACTTTGGCATTGTGGAAGG	ACACATTGGGGGTAGGAACA
Endoglin	CTTCCAAGGACAGCCAAGAG	GTGGTTGCCATTCAAGTGTG
IL-7	ACAGCCAGAGGAGTTGGAGA	GGGCTGACTGAAGTCTCAGG
MMP-9	TACAGGGCCCCTTCCTTACT	TGCCTGTGTACACCCACATT
IL-8	CGGCAATGAAGCTTCTGTAT	CCTTGAAACTCTTTGCCTCA
TNFα	TAGCCAGGAGGGAGAACAGA	TTTTCTGGAGGGAGATGTGG
CXCR2	AGCAGAGGATGGCCTAGTCA	TCCACCTACTCCCATTCCTG
BMP-6	AGCACAGAGACTCTGACCTATTTTTG	CCACAGATTGCTAGTTGCTGTGA
CXCL1	ACTGCACCCAAACCGAAGTC	TGGGGACACCTTTTAGCATCTT
CCL2	AGCACCAGCCAACTCTCACT	CGTTAACTGCATCTGGCTGA
IL-2	AAGCTCTACAGCGGAAGCAC	ATCCTGGGGAGTTTCAGGTT
IL-6	GTATGAATAACGATGATGCACTTG	ATGGTACTCCAGAAGACCAGAGGA
IL-10	CCAGGGAGATCCTTTGATGA	AACTGGCCACAGTTTTCAGG
PDGF-β	TTTGGAGACTTGGGCTGGGA	ACGGACCCCCAGATCAGAA
IFNγ	GCTTTAACAGCAGGCCAGAC	GGAAGCACCAGGTGTCAAGT
SDF-1	GAAAGGAAGGAGGGTGGCAG	TCCCCGTCTTTCTCGAGTGT
CXCL2	ATCCAGAGCTTGAGTGTGACG	GTTAGCCTTGCCTTTGTTCAG
TGF-β1	CAACAATTCCTGGCGTTACC	TGCTGTCACAAGAGCAGTGA
TGF-β2	CCGCCCACTTTCTACAGACCC	GCGCTGGGTGGGAGATGTTAA
TGF-β3	GTTTGCAGCATTTGTGATCG	TGCTCTGAGTGCTCCCTATG
VEGF	ACCAGCGAAGCTACTGCCGT	TAACTCAAGCTGCCTCGCCT

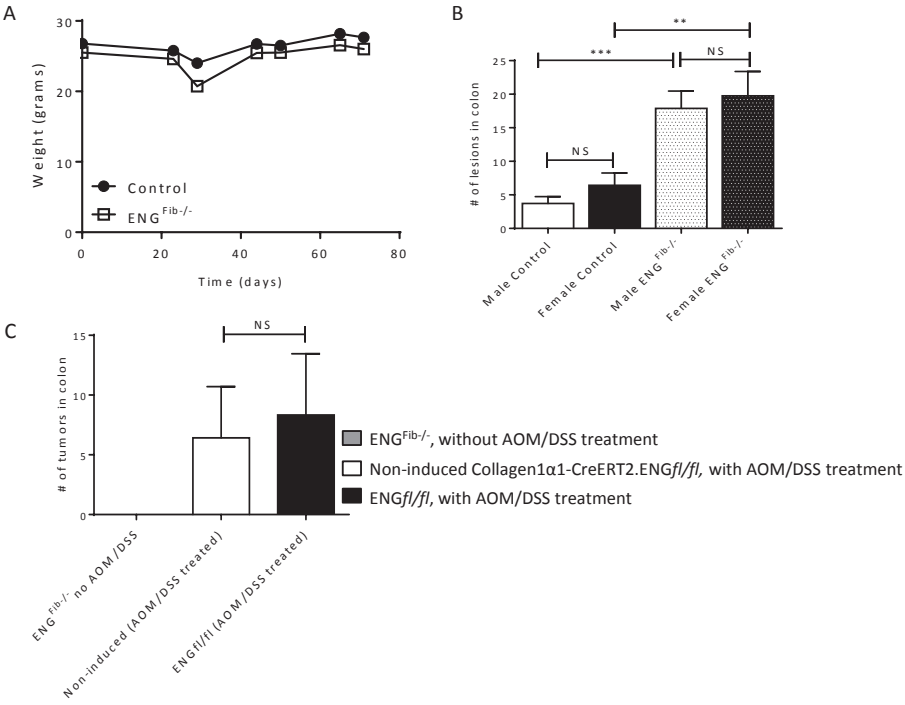

Supplementary figure S1. A. Mouse weights dropped during DSS supplementation, but recovered during the two weeks on normal drinking water. B. The number of lesions observed in the AOM/DSS model is independent of animal sex, in both the control and ENG$^{Fib-/-}$ group. C. Fibroblast-specific endoglin deletion without AOM/DSS treatment did not induce neoplastic growth over the course of 13 weeks (n=8). ENG*fl/fl* mice, which received tamoxifen, showed similar number of lesions as non-induced collagen1α1-CreERT2. ENG*fl/fl* mice after AOM/DSS (n=9).

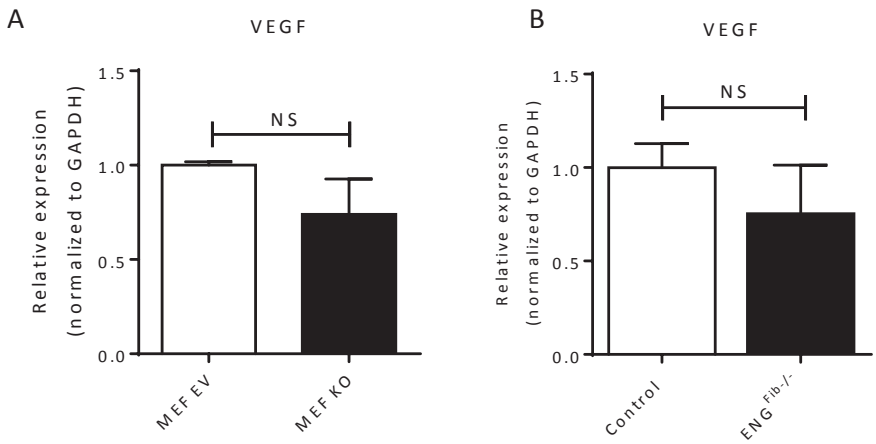

Supplementary figure S2. A. VEGF expression was determined by RT-qPCR and expression levels were not changed upon endoglin knock out in MEFs. B. VEGF mRNA levels were not changed in AOM/DSS-induced adenomas when endoglin was deleted in fibroblasts. Graph represents 9-5 lesion/group from two independent experiments.